STABILITY OF EPS SYSTEM OF AGRICULTURAL VEHICLES UNDER VIBRATION ENVIRONMENT

/

农用车辆振动环境下电动助力转向系统的稳定性研究

Ph.D. Zhipeng Li, M.S. Songzhuo Shi*)
School of Transportation, Northeast Forestry University, Harbin, Heilongjiang/ China
Tel: +86-0451-82191847; E-mail: sisongzhuo@126.com

Keywords: *road surface input; power steering; global fast terminal sliding mode control; steering stability*

ABSTRACT

Agricultural towing vehicles are driven under poor road conditions. The impact of rough road surface seriously affects the driving safety of agricultural towing vehicles. The mechanism of vibration of agricultural towing vehicles caused by rough roads is explored to reduce the adverse effects of road surface impact on the handling stability of agricultural towing vehicles and to improve the handling and steering stability of vehicles. First, the adverse effects of rough road input conditions on the handling stability of electric power steering (EPS) system were considered, and the kinetic model of the EPS system and the eight degree-of-freedom models of the whole vehicle were established. Second, tire and road surface impact models were introduced. Finally, the stability of the steering system under rough road input conditions was analyzed. Results show that the current following accuracy of the proposed motor control system is increased by 5%, and the final return-to-center residual angle of the steering wheel is 15 degrees. This study indicates that the vehicle vibration caused by road surface impact affects not only the driving stability of vehicles but also the smooth return of the steering system. The motor control system designed in this study effectively reduces the adverse effects of road surface impact on the steering system. The analysis and research process and the results are suitable for the investigation on the return-to-center performance of the EPS system for passenger and freight cars and the response of vehicle handling stability under different vibration sources.

摘要

农用牵引车辆行驶路面条件恶劣，路面不平产生的冲击严重影响了农用牵引车辆的行驶安全性。为了降低路面冲击对农用牵引车辆操纵稳定性造成的不良影响，本文研究了路面不平引起的农用牵引车辆振动的产生机理，以提高车辆转向时的操纵稳定性。首先，针对不平路面输入状况对电动助力转向系统操纵稳定性产生的不良影响，建立了电动助力转向系统动力学模型与整车 8 自由度模型，同时引入了轮胎和路面冲击模型，分析了不平路面输入状况下转向系统的稳定性。结果显示，本文设计的电机控制系统的电流跟随准确性提升了 5%，转向盘的最终回正残留角度为 。研究表明，路面冲击产生的车辆振动不仅对车辆的行驶稳定性产生影响，同时会影响转向系统转向回正平顺性，本文设计的电机控制系统有效降低了路面冲击对转向系统性能造成的不良影响。本文的分析和研究过程适用于研究乘用车及货运车电动助力转向系统回正性能和车辆操纵稳定性在不同振源下的响应，研究结论可以应用在不同路面激励下，电动助力转向系统转向盘回正响应的理论研究中。

INTRODUCTION

Agricultural towing vehicles have complex working conditions because roads in the wild field are rough, and these vehicles are prone to making lateral and yaw motion when steering. When the steering wheel of agricultural towing vehicles returns to center, road surface impact also affects the accuracy of the return-to-center angle of the steering wheel, thereby causing the vehicle to deviate from the safe travel path. The EPS system is combined with the active front-wheel steering system in which the damping compensation algorithm is used to control the power motor in the EPS system, to effectively reduce the negative effect of road surface impact on the steering system *(Fan lu and Zhou bing, 2014)*. The vibration sources of vehicles, such as the jitter that occurs when the engine is running, and the low-frequency vibration of the steering system itself, affect the steering stability of vehicles *(He Ren and Miao Lidong, 2009)*. In the research on road vibration, the road surface input model is divided into random and non-random road surface input models; currently, research on the road surface input model mainly focuses on

non-random road surface input model *(Hu Jianjun, et al., 2008)*. Scholars generally believe that the high-precision control algorithm of motor current tracking and the simulation technology of computer-based road vibration play a unique role in suppressing road vibration and improving EPS steering stability *(Hamada H. et al., 2006; Anthony J, 2000)*. Other scholars have also conducted considerable research to explore the improvement of the response speed and precision of motor used in the EPS system and to reduce the adverse effect of vehicle vibration on the motor tracking performance. Zhao and Bei *(Bei Shaoyi et al., 2011)* applied the fuzzy PID control algorithm to the return-to-center control to improve the return-to-center stability of the EPS system, and the experimental results indicated that the algorithm improves the insufficient and overshoot return-to-center situations of the steering system. Borowiec et al. *(Sen A. et al., 2010)* collected data on the vertical acceleration speed of left and right suspension racks of a vehicle under three road conditions, namely, asphalt, stone, and imitation railway crossroads; their analysis results of the collected data values showed that the vertical vibration of the suspension rack caused by roads is a low-frequency vibration. Múčka *(Múčka P, 2016)* used the "road surface vehicle driver" as a carrier and established the relationship between the international flatness index and road roughness impact response to improve the driving comfort and vehicle safety of the driver.This study analyzes the kinetic model of the EPS system, the road surface input model, and the eight degree-of-freedom (DOF) whole vehicle model, and investigates the effect of road surface impact on the steering stability of the EPS system.

MATERIAL AND METHODS

Eight DOF model of agricultural towing vehicles

Based on the yaw, lateral, and pitching motion of vehicles, the vehicle longitudinal dynamics of the four DOF mathematical model was established. Formulas 1-3 are the kinetic equation of the vehicle in the yaw, lateral, and pitching DOFs *(Xiao Hansong et al., 2014; Guo Konghui, 1991)*, respectively.

$$I_z\ddot{Y}_{aw} = \frac{B_1}{2}[(-F_{x11}+F_{x12})\cos¢ - (-F_{y11}+F_{y12})\sin¢] + \frac{B_2}{2}(-F_{x12}+F_{x22}) + a[(F_{x11}+F_{x12})\sin¢ + (F_{y11}+F_{y12})\cos¢] - b(F_{y21}+F_{y22}) \quad (1)$$

Where Y_{aw} is yaw angular velocity of vehicle (rad/s), $¢$ is steering angle of front wheel (°), a is distance between vehicle centroid and front wheels(mm), b is distance between vehicle centroid and rear wheels (mm), B_1 and B_2 is distance between front wheels and between rear wheels respectively (mm), I_z is vehicle yaw moment of inertia (kg/m^2), $F_{x11}, F_{x12}, F_{x21}$ and F_{x22} is lateral force of left front, left rear, right front, and right rear tire, respectively (N), F_{y11},F_{y12},F_{y21} *and* F_{y22} is longitudinal force of left front, left rear, right front, and right rear tire, respectively (N).

The pitch motion equation of vehicles is as follows:

$$J_y\ddot{¯} + m_sD_0(\dot{u} - v\dot{Y}_{aw}) - F_{s11}a - F_{s12}a + F_{s21}b + F_{s22}b = 0 \quad (2)$$

Where m_s is mass of the whole vehicle (kg), J_y is the pitch moment of inertia of the vehicle body (kg/m^2), $F_{s11}, F_{s12}, F_{s21}$ and F_{s22} is suspension force (N), v is vehicle horizontal velocity (m/s), $¯$ is vehicle pitch angle (°), u is vehicle lateral velocity (m/s^2), D_0 is coefficient of body roll.

The lateral motion equation of vehicles is as follows:

$$J_x\ddot{f} - m_se_0(\dot{v} + u\dot{Y}_{aw}) = -F_{s11}\frac{1}{2}B_{11} + F_{s12}\frac{1}{2}B_{11} - F_{s21}\frac{1}{2}B_{22} + F_{s22}\frac{1}{2}B_{22} \quad (3)$$

Where: J_x is vehicle lateral moment of inertia (kg/m^2), f is the roll angle of the vehicle, e_0 is coefficient of body pitch.

The vertical displacement caused by random road excitations will change the vertical force of vehicles. The vertical motion equation of vehicles is shown in Formulas 4-7.

$$m_{t1}\ddot{x}_{t1} = k_{t1}(x_{r1} - x_{t1}) + k_{s1}(x_{s1} - x_{t1}) + c_{s1}(\dot{x}_{s1} - \dot{x}_{t1}) \quad (4)$$

$$m_{t2}\ddot{x}_{t2} = k_{t2}(x_{r2} - x_{t2}) + k_{s2}(x_{s2} - x_{t2}) + c_{s2}(\dot{x}_{s2} - \dot{x}_{t2}) \quad (5)$$

$$m_{t3}\ddot{x}_{t3} = k_{t3}(x_{r3} - x_{t3}) + k_{s3}(x_{s3} - x_{t3}) + c_{s3}(\dot{x}_{s3} - \dot{x}_{t3}) \quad (6)$$

$$m_{t4}\ddot{x}_{t4} = k_{t4}(x_{r4} - x_{t4}) + k_{s4}(x_{s4} - x_{t4}) + c_{s4}(\dot{x}_{s4} - \dot{x}_{t4}) \quad (7)$$

where m_{t1}, m_{t2}, m_{t3} and m_{t4} is suspension mass (kg), x_{r1}, x_{r2}, x_{r3} and x_{r4} is Roda surface stimulus input (mm). x_{s1}, x_{s2}, x_{s3} and x_{s4} is suspension mass and displacement at the connection of suspension (mm), c_{s1}, c_{s2}, c_{s3} and c_{s4} is equivalent damping coefficient of left front wheel, left rear wheel, right front wheel and right wheel, k_{s1}, k_{s2}, k_{s3} and k_{s4} is suspension stiffness coefficient, k_{t1}, k_{t2}, k_{t3} and k_{t4} is tire stiffness.

The longitudinal displacement of vehicles will cause the change in vehicle suspension force. Formulas 8–11 are used to calculate the suspension force.

$$F_{s11} = K_1(x_{t1} - a^{-} + \frac{1}{2}B_{11}f) + C_1(x_{t1} - a^{\dot{-}} + \frac{1}{2}B_{11}\dot{f}) \quad (8)$$

$$F_{s12} = K_1(x_{t2} - a^{-} - \frac{1}{2}B_{11}f) + C_1(x_{t2} - a^{\dot{-}} - \frac{1}{2}B_{11}\dot{f}) \quad (9)$$

$$F_{s22} = K_2(x_{t3} - b^{-} + \frac{1}{2}B_{22}f) + C_2(x_{t3} - b^{\dot{-}} - \frac{1}{2}B_{22}\dot{f}) \quad (10)$$

$$F_{s21} = K_2(x_{t4} - b^{-} + \frac{1}{2}B_{22}f) + C_2(x_{t4} - b^{\dot{-}} + \frac{1}{2}B_{22}\dot{f}) \quad (11)$$

where x_{t1}, x_{t2}, x_{t3} and x_{t4} is sprung mass displacement (mm).

Formula 12 expresses the conversion relationship between the steering and the front-wheel angle.

$$¢ = \frac{\bar{}_s}{n} - \frac{M_{l1} + M_{l2}}{k} \quad (12)$$

where M_{l1} and M_{l2} is positive moments of left and right front wheels (kg), k is stiffness of steering system, n is total transmission ratio of steering system.

The DOF of the whole vehicle model is illustrated in Fig.1.

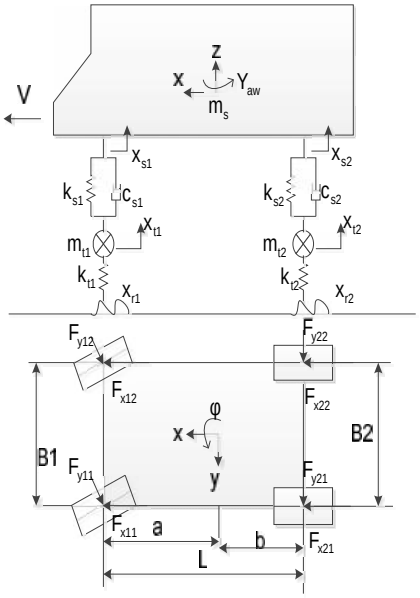

Fig.1 - Whole vehicle model

Kinetic model of EPS system

The EPS system is a steering column EPS system *(Lin Yi et al., 2007; Mohammadi H and Kazemi R, 2003)*, and the established kinetic equation of the EPS steering system is expressed as Formulas 13–17.

$$Steering\ column: J_s\ddot{\bar{}}_s + B_s\dot{\bar{}}_s + k_s(\bar{}_s - \frac{x_r}{r_p}) = T_d \quad (13)$$

$$Output\ shaft: J_e\ddot{e} + B_e\dot{e} = k_s(\bar{}_s - \frac{x_r}{r_p}) + \frac{k_m i_m}{r_p}(\bar{}_m - \frac{x_r}{r_p}) \quad (14)$$

$$Rack: m_r\ddot{x}_r + b_r\dot{x}_r + F_r = \frac{k_s}{r_p}(\theta_s - \frac{x_r}{r_p}) + \frac{k_m i_m}{r_p}(\theta_m - \frac{x_r}{r_p}) \quad (15)$$

$$Motor: J_m\ddot{\theta}_m + B_m\dot{\theta}_m = T_m - \frac{T_a}{G} \quad (16)$$

$$Motor\ current: i_m = \frac{u - k_m\dot{\theta}_m}{R} \quad (17)$$

where J_e is deceleration mechanism inertia (kg/m^2), J_m is motor moment of inertia (kg/m^2), B_s is damping coefficient of steering column, B_e is damping coefficient of deceleration mechanism, B_m is motor damping coefficient, k_s is stiffness coefficient of torque sensor, k_m is motor torque coefficient, T_m is motor electromagnetic torque (N.m), T_a is power torque of motor (N.m), T_d is input torque of steering wheel (N.m), x_r is rack displacement (mm), r_p is pinion radius (mm), i_m is motor current (A), m_r is total mass of pinion and rack (kg), b_r is sticking coefficient of the rack; G is transmission ratio of deceleration mechanism; U is motor voltage (V), F_r is force of tire on the road (N) , J_s is moment of inertia of steering column (kg/m^2).

Tire Model

The conversion between steering and the front wheel angle requires using the return-to-center torque of the tire; thus, introducing the tire mechanics model is necessary. The establishment of a relatively perfect tire model is difficult because the force of the tire is influenced by many factors, such as tire material, pressure, and positioning parameter. This study quotes a mature tire model, namely, the tire magic formula model *(Li Songyan et al., 2009)*.

In formula 18, F_r is the force between tire and road surface. If the tire sideslip angle is less than 3°, then the lateral force is linearly proportional to the transverse displacement of the rack x_r .

$$F_r = D\sin\{C\arctan[Bx - E(Bx - \arctan Bx)]\} \quad (18)$$

where Y is a longitudinal force, lateral force, or return-to-center torque; x is the tire sideslip angle or longitudinal slip rate; D is the peak factor; C is the shape factor; B is the stiffness factor and E is the curvature factor.

Under pure rolling conditions, the lateral force applied on the tire is expressed as follows:

$$F_y = D\sin\{C\arctan[BX_1 - E(BX_1 - \arctan BX_1)]\} + S_v \quad (19)$$

where S_v is the vertical displacement of the tire lateral force curve. Road surface conditions affect the smooth driving of vehicles, and the dynamic load of the tire is closely related to road excitation.

Road time-domain model of four-wheel input

The road-surface input model *(Lu Shifu and Zhao Heng, 1999)* acting on the tire is expressed as follows:

$$\dot{x}_r(t) = F_w x_0(t) + B_0 w_1(t) \quad (20)$$

where $x_r = [x_{r1}, x_{r2}, x_{r3} \text{ and } x_{r4}]^T$ is the road excitation input of four wheels. $w_1(t)$ is the white noise input of the left front wheel. F_w is the product of vehicle speed V and road roughness coefficient a.

Determination of return-to-center status of EPS system

The torque sensor used in the designed EPS system integrates the function of detecting the steering wheel angle. Therefore, the return-to-center conditions of the EPS system can be judged by the steering wheel angle and the change rate of angle. The judgment bases are demonstrated as follows:

Power control conditions: $\theta_s > 0, \dot{\theta}_s > 0$;

Return-to-center control conditions: $\theta_s > 0, \dot{\theta}_s < 0$;

Design of variable structure controller of global fast terminal sliding mode

A global fast terminal sliding mode control *(SMC)* can make the system *(Liu Jinkun, 2000)* state converge to zero within a finite time, whereas an ordinary sliding mode control gradually converges under the linear sliding mode surface. The dynamic performance of the system is better than the ordinary sliding mode control.

Design of sliding mode surface

The EPS system is a two-order system, and the sliding mode surface equation of the sliding mode controller is $s = \sim e + \dot{e} + \ e^{q/p}$, where $e = \bar{}_s - x_r$, $\dot{e} = \dot{\bar{}}_s - \dot{x}_r$, where e is the error signal, $\bar{}_s$ is the steering wheel angle, the state variable x_r is the displacement of gear, and α is the constant larger than zero and satisfies the Hurwitz polynomial. $b > 0$, p and $q\,(p > q)$ are positive odd number, in which $F(t)$ represents the non-linear part, $F(t) = f(t)\ e^{q/p}$. The sliding mode surface equation satisfies the following conditions: (1) $s(0) = \sim e(0) + \dot{e}(0) + F(t)$; (2) $t \to \infty, s(0) = 0$; (3) $s = \sim e + \dot{e} + \ e^{q/p}$ and can be differentiable. Condition (1) ensures that the initial condition of the system is on a sliding mode surface. Condition (2) ensures the gradual stability of the system. Condition (3) ensures the occurrence of sliding mode motion.

Verifying the stability of sliding mode controller

The high-order single-input single-output nonlinear state equation of the global fast terminal sliding mode controller is expressed in the following formulas:

$$\dot{x}_i = x_{i+1} \tag{21}$$

$$\dot{x}_n = f(x) + g(x)u(t) \tag{22}$$

According to the sliding mode surface equation, the recursive expression for the sliding mode surface of the global fast sliding mode is expressed as follows:

$$s_{n-1} = \dot{s}_{n-2} + \sim_{n-2} s_{n-2} + \ _{n-2} s_{n-2}^{\ q_{n-2}/p_{n-2}} \tag{23}$$

According to formula 23,

$$\dot{s}_{n-1} = \ddot{s}_{n-2} + \sim_{n-2} \dot{s}_{n-2} + \ _{n-2} \frac{d}{dt} s_{n-2}^{\ q_{n-2}/p_{n-2}} \tag{24}$$

$$\dot{s}_{n-1} = f(x) + g(x)u(t) + \sum_{k=0}^{n-2} \sim_k s_k^{(n-k-1)} + \sum_{k=0}^{n-2} \ _k \frac{d^{n-k-1}}{dt^{n-k-1}} s_k^{q_k/p_k} \tag{25}$$

After substituting formula 2 into formula 25,

$$\dot{s}_{n-1} = \text{-}\ddot{}\, s_{n-1} \text{-} ¥ s_{n-1}^{q/p} \tag{26}$$

According to Lyapunov function,

$$V = \frac{1}{2} s_{n-1}^2 \tag{27}$$

Then, $\dot{V} = s_{n-1}\dot{s}_{n-1} = \text{-}\ddot{}\, s^2_{\ n-1} \text{-} ¥ s_{n-1}^{(q+p)/p}$, $p+q$ is an even number; thus, when $\dot{V} < 0$, the system is stable.

Design of sliding mode control rule

If $x = \bar{}_s$, then the EPS system model can be represented by a high-order single-input single-output nonlinear system:

$$\ddot{x} = f(x) + g(x)u(t) + d(t)$$

$$f(x) = (\frac{k_m^{\ 2} G_m}{R} + \frac{k_m^{\ 2} p G_m}{J_s r_p})x - (B_s + \frac{k_m^{\ 2} G_m^{\ 2}}{R})\dot{x}; \quad g(x) = -\frac{k_m G_m}{R} x - \frac{k_m x_r}{J_s r_p}; \tag{28}$$

$$d(t) = \frac{T_d}{J_s} - \frac{r_p}{J_s}(m_r \ddot{x}_r + b_r \dot{x}_r + k_r x_r)$$

The control rule of the global time-varying sliding mode, $u = u_{eq} + u_{vss}$, $\ddot{x} = f(x) + g(x)u(t) + d(t)$ is substituted into $\dot{s} = 0$. Then,

$$u = \frac{\sim \dot{e} + \ qe + p[\frac{k_m G_m}{R} x - (B_s + \frac{k_m^{\ 2} G_m^{\ 2}}{R})\dot{x}}{\frac{k_m G_m}{R} x + \frac{k_m x_r}{J_s p}} + K sign(t) + \frac{k_m^{\ 2} p \bar{}_m^{\ 2} - \frac{r_p}{J_s}(m_r \ddot{x}_r + b_r \dot{x}_r + k_r x_r)}{\frac{k_m G_m}{R} x + \frac{k_m x_r}{J_s p}} \tag{29}$$

RESULTS

In this study, an LH-UTV-400 low-energy-consumption agricultural towing vehicle is used as the research object. Fig.2(a) depicts the real vehicle.

Table 1 displays the measurement parameters of the vehicle.

Fig. 2(a) - Picture of vehicle

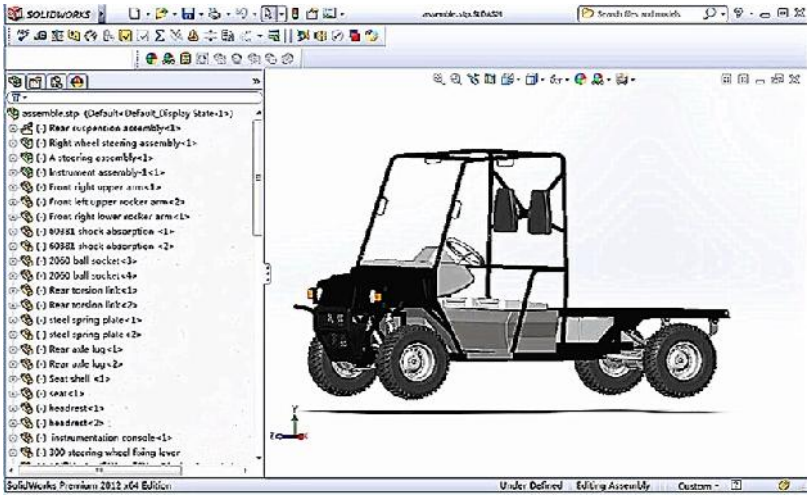

Fig.2(b) - Picture of vehicle model

Fig.2(b) illustrates the vehicle simulation model established in SolidWorks software based on the measurement parameters of the vehicle.

Table 1

Vehicle parameters

Name of parameters	Parameter value
Mass of vehicle, (m/kg)	3021
Mass of suspension, (m_s/kg)	2687
Lateral inertia moment of body, (J_x/kg/m^2)	1960
Distance between front wheels, B_1 (mm)	1320
Distance between rear wheels B_2 (mm)	1330
Distance between vehicle centroid and front axle, a (m)	1.24
Distance between vehicle centroid and rear axle b (m)	1.28
Body yaw rotation inertia I_x (kg/m^2)	10437
Mass of front wheel non-suspension, m_{t1}, m_{t2} (kg)	55
Mass of rear wheel non-suspension, m_{t3}, m_{t4} (kg)	58
Stiffness of front suspension k_{s1}, k_{s2} (N/m)	17000
Stiffness of rear suspension k_{s3}, k_{s4} (N/m)	2000
Total transmission ratio of steering system, n	18
Stiffness of left-front tire and left rear-tire k_{t1},k_{t2} (N/m)	192000
Stiffness of left-front tire k_{t3} and left-rear tire k_{t4} (N/m)	192000
The total stiffness of the steering system k (N/m)	2317
The damping coefficients of left-front wheel and left-rear wheel c_{s1} c_{s2} (Ns/m)	2048
The damping coefficients of right-front wheel and right-rear wheel c_{s3} and c_{s4}(Ns/m)	2048

Comparison between accuracy of motor target current tracking through the variable structure control algorithm of the global fast terminal sliding mode and PID algorithm

The preconditions for the variable structure controller of the global fast terminal sliding mode to reach the steady state include the following: (1) The sliding mode surface moves on the surface s = 0 from t = 0. (2) The phase trajectory of the system finally converges to 0. In Fig.3, the sliding mode surface selected by global fast terminal sliding mode control has a position displacement of −0.1 near s = 0 at the initial stage of the system motion, which lasts for approximately 0.25 s, and the state variable selected from the system moves on the sliding mode surface s = 0. In Fig.4, the phase plane of the sliding mode controller is convergent, indicating that the sliding mode control is stable. The motion trajectory of the state variable selected by the sliding state controller has been on the sliding mode surface, and the system has strong robustness. Therefore, applying the sliding-mode control algorithm in the motor control system is essential to enhance the control accuracy of the EPS system.

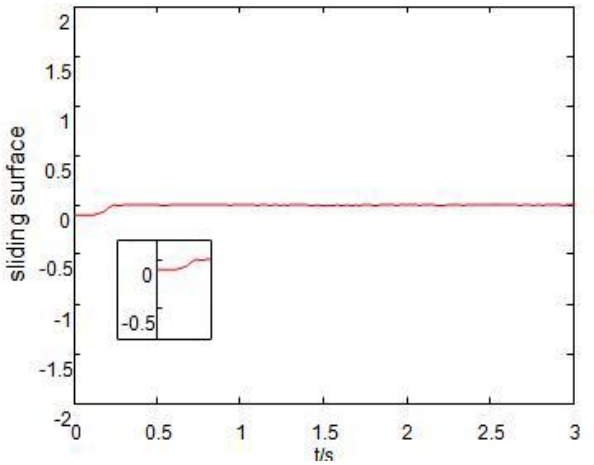

Fig. 3 - Sliding mode surface

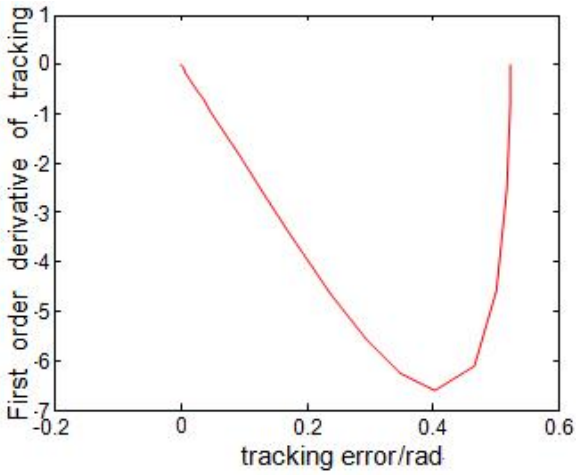

Fig. 4 - Phase trajectory

After adding the control algorithm of the global fast sliding mode into the EPS system, the tracking accuracy of the motor target current is increased by 5%. In Fig.6, the control algorithm of the global fast sliding mode increases the robustness of the system and weakens the jitter effect of the road surface impact on the motor current. In Fig.5, the traditional PID algorithm has obvious inadequate motor current tracking effect, whereas the motor current has a significant jitter. The effect of road surface impact is retained.

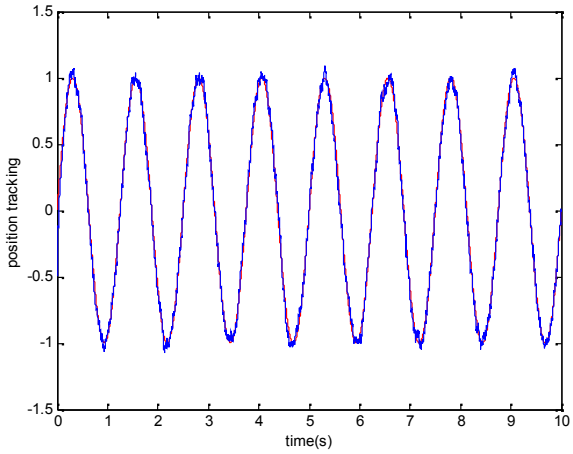

Fig. 5 - Traditional PID control

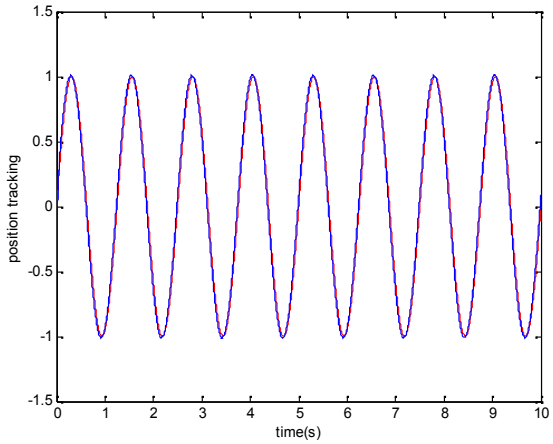

Fig. 6 - Global fast sliding mode control

Relationship between vehicle handling stability and road surface impact

Based on the simulation model of "road surface–EPS system vehicle," this study compares the response curves of the yaw angular velocity with the lateral acceleration by using the sliding mode and the PID control and concludes that the yaw angular velocity response of the vehicle controlled by the global fast sliding mode control is zero under road surface impact, and the yaw angular velocity response residual of vehicle is 0.01 under control of traditional PID. The results indicate that the global sliding mode control can effectively overcome the impact of road direction input on the yaw angular velocity of the vehicles.

Fig.7 indicates the response of yaw angular velocity and Fig.8 indicates the response of lateral angular velocity.

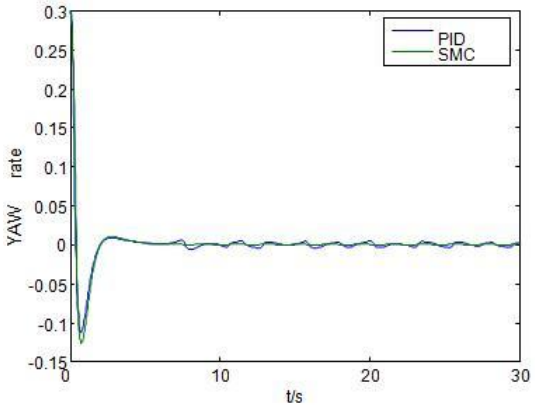

Fig. 7 - Response of yaw angular velocity

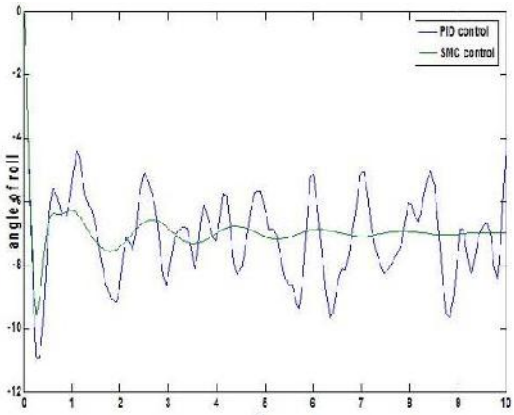

Fig. 8 - Response of lateral angular velocity

According to the judgment basis of the return-to-center conditions of the EPS system, Fig.9 analyzes the return-to-center residual angle of the steering wheel.

The results indicate that the steering-wheel residual angle of the EPS system that is added with the return-to-center control is 15°. This steering wheel angle does not cause a jitter phenomenon. Meanwhile, the steering-wheel residual angle of the EPS system that excludes the return-to-center control is 40°. This steering wheel angle generates significant jitter because of the effect of road surface impact.

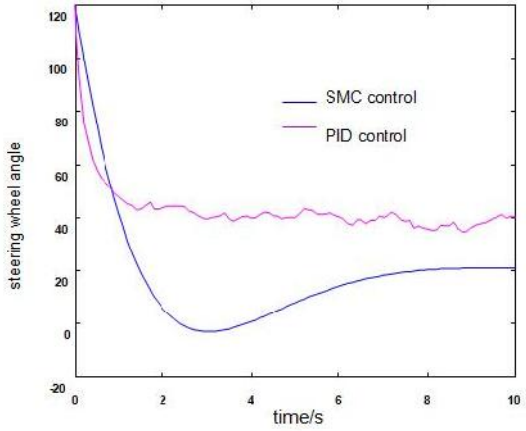

Fig. 9 - Diagram of steering wheel return-to-center results

CONCLUSIONS

In order to reduce the adverse effects of road surface impact on the handling stability and the smooth return-to-center of agricultural towing vehicles, the LH-UTV-400 low-energy-consumption agricultural towing vehicle was taken as research object, a road surface impact model was established, road surface impact model was combined with the whole vehicle model, the global fast terminal sliding mode control algorithm was added into the EPS control system, and a complete simulation model of “road surface - vehicle-EPS system” was established.

Finally, the main conclusions are presented below:

- when agricultural towing vehicles were steering, road surface impact increases the amplitude of the yaw motion and lateral motion of vehicles, and reduces the driving stability of vehicles.
- when steering wheel returns to center, the vibration caused by road surface impact was transmitted to steering wheel, resulting in the slight jitter of steering wheel, and reducing the stability of steering system. After global fast terminal sliding mode control algorithm was added into motor control algorithm, the tracking accuracy of motor current was improved significantly. After the steering wheel returns to the basic middle of angle, the return-to-center process of steering wheel was more smooth and stable.
- global fast terminal sliding mode control algorithm could make the power motor of the EPS system respond quickly to different steering conditions, improved the steering performance of vehicles in the condition of road excitation input, and it had great engineering practice significance in improving the steering stability of vehicles.

The steering stability response of the EPS system for agricultural towing vehicles under road surface impact is investigated, a motor current tracking control algorithm based on the global fast terminal sliding mode variable structure control algorithm is proposed, the accuracy of tracking and controlling motor current is improved, the return-to-center angle of steering wheel is calculated more accurately, and the jitter of steering wheel is weakened. Due to the limitations of models, the road surface impact investigated by this research is small-amplitude high-frequency impact. Based on this research, the influence of low-frequency large-amplitude road surface impact on the EPS system's return-to-center stability will be explored in future research, and the whole vehicle model will be further improved in the future.

ACKNOWLEDGEMENT

The work was supported by supported by the Fundamental Research Funds for the Central Universities (2572015AB19)

REFERENCES

[1] Bing Zhou, Lu Fan, (2014), Integrated control of EPS and AFS to reduce steering vibration derived from road impact. *China Mechanical Engineering*, Vol.25, Issue 22, Editorial Department of China Mechanical Engineering, Wuhan, pp.3114-3118;

[2] Champagne A., (2000), Correlation of Electric Power Steering Vibration to Subjective Ratings. *2000 SAE World Congress*, Vol.20, Issue 6, SAE International, Pittsburgh, pp.1-5;

[3] Datong Qin, Jianjun Hu, Tong Li, (2008), Modeling and Simulation of Electric Power Steering System Based on Vehicle Whole Dynamics. *Journal of System Simulation*, Vol.20, Issue 6, Beihang University PRESS, Peking, pp.1577-1581;

[4] Guobiao Shi, Rongwei Shen, Yi Lin, (2007), Model and simulation of electric power steering system, *Journal of Jilin University (Engineering and Technology Edition)*, Vol.37, Issue 1, Editorial Department of Journal of Jilin University, Changchun, pp.31-36;

[5] Hamada H, Kurishige M, Sugiyama A et al., (2006), An EPS control strategy to reduce steering vibration associated with disturbance from road wheels, *2000 SAE World Congress*, Vol.20, Issue 6, SAE International, Pittsburgh, pp.1-5;

[6] Hansong Xiao, Linfeng Zhao, Qidong Wang, (2014), Vehicle system dynamics and integrated control, vol.1, Science press Ltd., Peking, pp.102-113;

[7] Heng Zhao, Shifu Lu, (1999), A vehicle's time domain model with road input on four wheels, automotive engineering, Vol.21, Issue 2, AutoFan magazine Ltd., Peking, pp.112-117;

[8] Jinkun Liu, (2000), *MATLAB Simulation for Soliding Model Control*, vol.1, Tsinghua University Press, Peking, pp.360-370.

[9] Kazemi R, Mohammadi H, (2003), Simulation of different types of electric power assisted steering (EPS) to investigate applied torque positions' effects, *2003 SAE World Congress*, Vol.20, Issue 6, SAE International, Pittsburgh, pp.1-5;

[10] Konghui Guo, (1991), *Vehicle Handling Dynamics*, vol.1, Jilin Science and Technology Press, Changchun, pp.183-200;

[11] Long Chen, Jingbo Zhao, Shaoyi Bei, (2011), Fuzzy-PID Control and Test of Automotive EPS System Under Return-to-center Condition. *Journal of Zhengzhou University (Engineering Science)*, Vol.32, Issue 5, Editorial Department of Journal of Zhengzhou University (Engineering Science), Zhangzhou, pp.112-116;

[12] Lidong Miao, Ren He, (2009), Analysis of vibration modes for electric power steering system. *Journal of Jiangsu University*, Natural Science Edition, Vol.30, Issue 4, Editorial Department of Journal of Jiangsu University (NATURAL SCIENCE EDITION), Nanjing, pp.362-365,391;

[13] Liangmo Wang, Songyan Li, Yongjun Min, (2009), Establishment and Simulation Analysis of Tire Dynamic Model, *Journal of Nanjing Institute of Technology (Engineering and Technology Edition)*, Vol.7, Issue 3, Editorial department of journal of Nanjing institute of technology, Nanjing, pp.34-38;

[14] Múčka P., (2016), Road Roughness Limit Values Based on Measured Vehicle Vibration. *Journal of Infrastructure Systems ,*Vol.10, Issue 6, ASCE, Reston, pp.1-23;

[15] Sen A.K., Niewczas A, Litak G. etc., (2010), Vibrations of a vehicle excited by real road profiles, *Forschung im Ingenieurwesen*, Vol.74, Issue 2, Pamm, Darmstadt, pp.99-109.